

## Broadening of the excitonic mobility edge in a macroscopically disordered CdSe/ZnSe short-period superlattice

A. A. Toropov, T. V. Shubina, S. V. Sorokin, A. V. Lebedev, R. N. Kyutt,  
and S. V. Ivanov

*Ioffe Institute of RAS, Politechnicheskaja 26, 194021 St. Petersburg, Russia*

M. Karlsteen and M. Willander

*Physical Electronics and Photonics, Department of Microelectronics and Nanoscience, Chalmers University of Technology  
and Göteborg University, S-412 96 Göteborg, Sweden*

G. R. Pozina, J. P. Bergman, and B. Monemar

*Department of Physics and Measurement Technology, University of Linköping, S-581 83 Linköping, Sweden*

(Received 21 September 1998)

Selective excitation photoluminescence measurements performed in CdSe/ZnSe superlattices with an embedded  $\text{Zn}_{1-x}\text{Cd}_x\text{Se}$  quantum well reveal the limitation of the mobility edge concept to describe the dynamics of localized excitons in this system. Both localized and extended excitonic states are found to coexist in a certain energy range. We suggest that this behavior is governed by a macroscopic band-gap modulation imposed on the microscopic random localization potential. [S0163-1829(99)50704-2]

It is currently widely accepted that the relaxation dynamics of excitons in a random potential arising either from local compositional fluctuations in mixed semiconductor alloys or from quantum well (QW) thickness fluctuations (or from both simultaneously) can generally be described in the Mott-Anderson localization model.<sup>1</sup> A key point of this model is the idea of a mobility edge, which is a sharp boundary separating the energy spectra of localized and delocalized particles. Two obvious restrictions on the applicability of this approach to localized excitons in semiconductors have been formulated already in early papers.<sup>2,3</sup> The first is the question of time scale. The Mott-Anderson model assumes an infinite carrier lifetime, whereas excitons in direct-gap semiconductors only live for about 1 ns or less. Therefore, an “effective” mobility edge had to be introduced, defining delocalized excitons as those with the localization length of the same order as the diffusion length. The second complication is that the Mott-Anderson picture of a well-defined mobility edge assumes that the disorder is of “microscopic” origin. If this is not the case, the states of the same energy might be localized in one “macroscopic” part of the crystal and delocalized in another, without any possibility to communicate with each other. In spite of these restrictions, many experimental results on the dynamics of localized excitons both in bulk alloy samples<sup>2,4,5-7</sup> and in two-dimensional (2D) QW systems<sup>3,8,9-11</sup> of different semiconductors have been successfully interpreted in terms of the effective mobility edge concept. Furthermore, to the best of our knowledge, no experimental measurements have been so far reported, directly suggesting that extended and localized excitonic states of comparable densities may coexist at the same energy within the same disordered semiconductor medium.

In this paper, we combine the results of low-temperature cw and time-resolved selective excitation photoluminescence measurements in order to demonstrate that localized and delocalized excitons can coexist in the specific semiconductor

system within a quite extended energy range. A key experimental point in this study is a careful design of the sample structures, which contain short-period CdSe/ZnSe superlattices (SL's) with an embedded deeper  $\text{Zn}_{1-x}\text{Cd}_x\text{Se}$  QW (see Fig. 1 for a schematic view of the structure). There are several reasons for this choice. The structures containing the SL to be studied, with an enlarged test well to probe the carrier population, offer the unique possibility of measuring vertical transport by all-optical methods.<sup>12-16</sup> In our case, however, the deeper well rather introduces a kind of “escape mechanism,” allowing to control the tunneling lifetime of extended excitonic states in the SL. Furthermore, an advanced molecular beam epitaxy (MBE) technique has recently been developed, allowing the reproducible growth of fractional monolayer (FM) CdSe/ZnSe heterostructures with high structural quality and a predetermined degree of intrinsic structural disorder.<sup>17,18</sup> Finally, recent optical data on the CdSe/ZnSe FM SL's suggest self-organizing formation of 1 monolayer

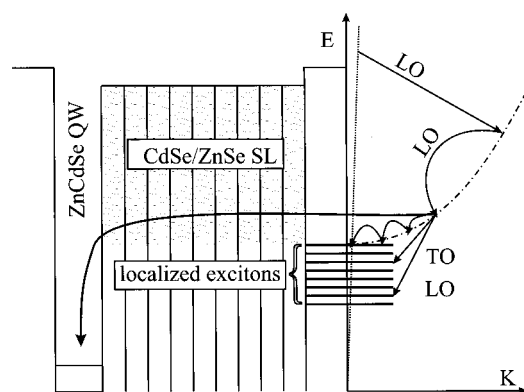


FIG. 1. Schematic illustration of exciton relaxation processes in a “SL+QW” sample. The dot-dashed line represents the dispersion of the  $1s$ -heavy-hole excitons and the dotted line is the photon dispersion.

(ML) height planar CdSe-based islands with lateral sizes exceeding the exciton Bohr radius.<sup>19</sup> As a result, one can expect spatial modulation of the band gap occurring on a “macroscopic” scale, probably exceeding the exciton diffusion length.

The samples used in this study were grown by MBE pseudomorphically to GaAs (100) substrates. The growth details have been reported elsewhere.<sup>17–19</sup> All the samples include a CdSe/ZnSe 10 period SL, differing in the SL average period ( $d$ ) and the CdSe average thickness ( $w$ ). In certain samples a 7-nm  $\text{Zn}_{0.77}\text{Cd}_{0.23}\text{Se}$  QW is attached to the SL from the substrate side. The whole intrinsic region is embedded in a thick layer of  $\text{Zn}_{1-x}\text{S}_x\text{Se}$  lattice matched to GaAs. The values of  $d$  and  $w$  for all the samples have been estimated from x-ray diffraction measurements.<sup>20</sup> The Stokes shift was measured in a set of samples ( $d \sim 30$  Å,  $w$  ranging from 0.05 to 2 ML) as the difference between the photoluminescence (PL) and PL excitation (PLE) peaks related to the lowest heavy-hole SL exciton. The shift, which can be considered as a measure of the disorder, is negligible at  $w < 0.5$  ML and increases rapidly when  $w$  exceeds this value. An additional characteristic of the disorder-induced localization for the samples with a  $\text{Zn}_x\text{Cd}_{1-x}\text{Se}$  deeper well is the ratio of the SL to QW integrated PL intensities. As it has been recently reported,<sup>21</sup> in the range  $w < 0.6$  ML ( $d \sim 30$  Å) the SL emission band is practically unobservable, due to the extremely efficient escape of carriers through the extended miniband states of the SL consisting, presumably, of homogeneous alloylike layers.<sup>18,22</sup> However, the SL emission band appears at  $w \sim 0.6$ – $0.7$  ML and rapidly increases in intensity with a further increase in  $w$ , reflecting an increase in structural disorder. This behavior allows one to modify almost independently the exciton localization strength (by a slight change of  $w$  in the range 0.6–1 ML) and the exciton tunneling escape rate (by variation of the SL average period  $d$ ). Cw PL experiments were carried out using a dye laser pumped by an  $\text{Ar}^+$  laser, and measurements of PL decay times were performed with a frequency-doubled beam of an  $\text{Al}_2\text{O}_3:\text{Ti}$  mode-locked laser and a syncroscan streak camera. The spectral and time resolution are estimated as 0.5 Å and 20 ps, respectively.

The excitonic PL spectrum of the SL samples without an embedded QW is in general similar to the spectra presented in Ref. 23. It consists of a background PL contour, with a shape independent of the excitation wavelength, superimposed with a small narrow peak exactly following the excitation, with the energy distance equal to an integer number of ZnSe LO phonons ( $31.9 \pm 0.1$  meV). However, the dominance of the nonresonant background signal prevents detailed studies of the optical-phonon-assisted resonant spectrum. The situation changes dramatically after embedding a deeper QW into the SL. The background contour almost disappears, revealing a complicated fine structure of the resonant part of the spectrum, as illustrated in Fig. 2 for the “SL+QW” sample with  $w = 0.81$  ML and  $d = 32$  Å. The cw PL spectra shown there correspond to the excitation energies around two ZnSe LO phonons above the SL heavy-hole excitonic peak visible in a PLE spectrum (dashed curve in Fig. 2) detected within the QW excitonic emission band. The phonon sideband displays a resonant enhancement within the excitonic contour and its shape is drastically dependent on

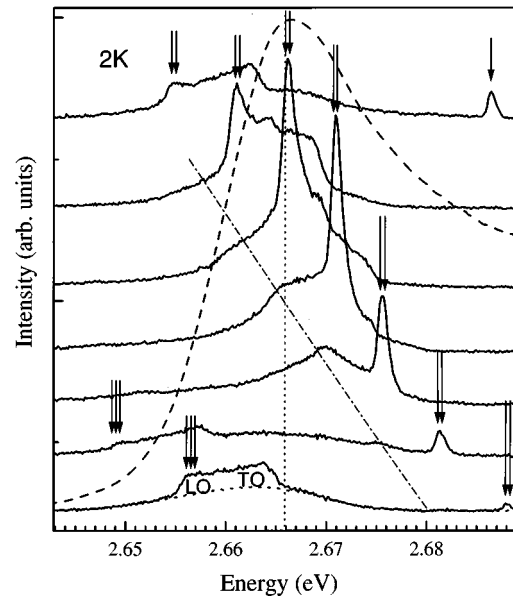


FIG. 2. Selective excitation cw PL spectra (solid curves) measured in the “SL+QW” sample with  $w = 0.81$  ML and  $d = 32$  Å. The spectra are vertically offset for clarity. Single, double, and triple vertical arrows point to the energies detuned from the excitation by one, two, or three ZnSe LO phonons, respectively. The dotted curve at the lowest spectrum represents an example of the nonresonant background contribution. The dashed curve is a PLE spectrum detected within the  $\text{Zn}_{1-x}\text{Cd}_x\text{Se}$  QW emission band.

the position relative to the PLE peak maximum. Above a certain demarcation energy (marked in Fig. 2 by a dotted vertical line) close to the center of the PLE peak, a single sharp line related to the ZnSe LO phonon is dominant in the PL spectrum. Below this energy the sideband is wider, containing a few narrow lines. The low-energy boundary peak is placed exactly at an integer number of ZnSe LO phonons below the excitation energy, whereas the higher-energy sideband boundary rather keeps a constant gap ( $\sim 25$  meV) with respect to the position of the nearest higher-energy LO-phonon-assisted line. As a result, the width of the resonant structure is  $\sim 7$  meV, independent of the sideband order (compare the lowest and uppermost PL spectra in Fig. 2).

To complete this introductory description, we note that the results of time-resolved PL measurements agree well with those reported for ZnSe/CdSe SL’s by Neukirch *et al.*<sup>23</sup> The PL rise time is noticeably shorter for the resonant features than for the smooth underlying background contour (the available time resolution in our experiments is not enough to measure it accurately). The decay times are essentially the same for resonant lines and the background spectrum at any wavelength, being as long as 200–250 ps within the low-energy tail of the spectrum. Efficient spectral diffusion is observed within the background contour. Note that the shape of the nonresonant background contour is independent of the excitation energy and is consistent with that obtained for excitation above the  $\text{Zn}_{1-x}\text{S}_x\text{Se}$  barriers, in which case no sharp resonant features are observed. This nonresonant contribution is also visible in the cw PL spectra (see the dotted curve at the lowest spectrum in Fig. 2).

These findings allow one to determine the main aspects of the involved energy relaxation process, which is schemati-

cally shown in Fig. 1. A monochromatically excited population of “hot” excitons relaxes to states with a smaller in-plane wave vector, predominantly by emission of one or more LO phonons. If the hot exciton cascade finishes within the tail of localized states, direct creation of a narrow distribution of localized excitons is possible, leading to the observation of narrow fluorescence lines.<sup>2</sup> However, in our sample the density of localized states is relatively small (as governed by the choice of  $w$ ). Therefore, a narrow distribution of *free* 1 s excitons is created at the preceding step of the relaxation cascade, ending in the region with high density of extended excitonic states. As recently shown,<sup>24</sup> such a free-exciton distribution may remain nonthermal for up to  $\sim 100$  ps. Different mechanisms compete in the free-exciton thermalization following the initial fast relaxation cascade. The fastest one is accompanied by emission of an optical phonon (it occurs on the subpicosecond timescale). This process results in appearance of the multiple-line phonon sideband within the tail of localized excitons. Note that observation of additional optical-phonon modes, forbidden by momentum conservation for *free* excitons, is not surprising for the luminescence tail, since different phonons may couple to *localized* states.<sup>5,25</sup> Tentatively we assign the multiple-line structure to ZnSe LO and TO phonons, and interface phonon modes in between. However, the real situation can be even more complicated, involving ZnSe-like optical phonons from different critical points of the Brillouin zone. No CdSe-like phonons are expected, due to the low average amount of CdSe in the submonolayer structures. Concerning our experiments, formation of the intermediate free-exciton nonthermal distribution seems to be the only possibility to explain the fact that the optical-phonon-assisted narrow lines visible within the tail of localized states are connected to the neighboring LO-phonon-assisted sideband rather than to the respective excitation energy. Otherwise, assuming independent relaxation cascades for each type of optical phonons, the width of the sideband should be enhanced with an increase in the number of phonons involved.

Another relaxation process destroying the free-exciton distribution is assisted by emission of acoustical phonons. This mechanism is spectrally nonselective and, therefore, the density of available final states is much larger. As a consequence, this process, while being slower than that assisted by optical phonons, can also be important, depending on the contribution from other decay mechanisms. In particular, fast tunneling escape of free excitons through the short-period SL, followed by their trapping in the QW, makes the relatively slow (few tens of ps) acoustical-phonon-assisted relaxation quite inefficient, leading to the drastic decrease in the background smooth PL signal. In contrast to that, the exciton relaxation driven by acoustical phonons is dominant in the SL’s without a deeper QW. The lifetime of free excitons there is not limited by the artificial escape mechanism and the spectrally nonselective relaxation process enables a homogeneous filling of localized states, giving rise to the “background” PL contour. This nonresonant part of the PL signal is of pure excitonic (not free-carrier) nature, which is confirmed by observation of its thresholdlike disappearance when exciting resonantly below the “demarcation” energy, which resembles in many aspects an effective excitonic mobility edge.

Summarizing the previous discussion, most of the presented observations may be approximately explained in terms of the effective mobility edge concept, and it seems like even the position of the mobility edge can be explicitly determined (vertical dotted line in Fig. 2). Indeed the excitons below this energy demonstrate an ability to couple with phonon modes forbidden for free excitons, and their PL kinetics is specific for hopping relaxation within the tail of localized states.<sup>11,23</sup> On the other hand, the excitonic states above this energy are generally extended, which is confirmed by the dominant fast tunneling escape towards the deeper QW in the “SL+QW” structures. The lifetime of these mobile hot excitons is small, as governed by competition of four mechanisms: (i) fast spectrally selective localization assisted by emission of an optical phonon, (ii) spectrally nonselective relaxation assisted by acoustical phonons, (iii) radiative recombination, and (iv) tunneling escape towards different trapping centers, either artificial (like an embedded deeper QW) or natural (defect-induced centers with a fast nonradiative recombination). In the sample studied the lifetime is less than 20 ps, as limited by the available experimental time resolution.

Nonetheless, there are other observations that cannot be explained in this framework. Let us examine in more detail the PL spectra in Fig. 2. An additional line clearly appears 5–10 meV below the LO-phonon-assisted peak, when it approaches the “mobility edge” from higher energies. The course of this line with a variation of the excitation energy is shown in Fig. 2 by a dot-dashed line. Below the “mobility edge” it merges into the phonon sideband, converting further to a small smooth shoulder. The shape of the line is generally smooth, which suggests a relatively slow exciton relaxation assisted by acoustical phonons. Moreover, there are no optical phonons in the CdSe/ZnSe system, which could fit the line energy. The peak emerges above the “mobility edge” and also above the background PL contour attributed to the equilibrium distribution of thermalized localized excitons. It means that the line results from the metastable population of excitons, which are for some reason withdrawn from both the tunneling escape along the SL growth axis and the lateral diffusion accompanied by thermalization towards the equilibrium distribution.

The description of exciton luminescence from fluctuation-induced tails, performed in the framework of continuum percolation theory,<sup>6</sup> predicts that the emission primary results from isolated localized states, or from complexes of such states (superclusters) of a minimum size, because these states have a limited access to the transitions between the tail states and, hence, possess longer lifetimes. The localized states located above the “mobility edge” might be of two kinds. States of the first type arise from macroscopic regions characterized by a systematically larger band gap. These states are essentially similar to all other localized excitons but their spectrum is energetically shifted. The other type is represented by well-developed “superclusters” isolated from the rest of the medium by a macroscopic barrier. These states represent an intermediate between true localized and extended states and can demonstrate properties inherent for both types. Emergence of the states of both types requires a band-gap modulation occurring on the scale of the exciton diffusion length. Introduction of macroscopically isolated re-

gions could easily be achieved in the studied sample just allowing the CdSe constituent layers to possess “holes” (i.e., places where CdSe is replaced by the barrier ZnSe material) of lateral sizes comparable with the excitonic diffusion length. This situation can very well be generated during growth of these layers, characterized simultaneously by the submonolayer average delivery of the material and by a natural tendency to form complete monolayers. Moreover, emergence of such isolated regions agrees well with the model of configuration disorder, suggested for CdSe/ZnSe FM SL's in Ref. 19. Indeed, occurrence of laterally extended “holes” in one or more subsequent layers of the SL breaks up the vertical configuration of ten coupled QW's, characterized by the lowest possible exciton energy, into configurations of coupled QW's, which are (i) isolated from each other and (ii) characterized by the larger band-gap energy. These two conditions are obviously adequate to ensure observation of the “above mobility edge” localized states. Nevertheless, we cannot rule out a possible contribution from other mechanisms defining the macroscopic in-plane modulation of the SL band gap. In any case, the characteristic scale of the potential modulations should be comparable with the excitonic diffusion length (which is generally unknown for the

studied structures) or larger. A decrease in the excitation spot down to 0.1 mm does not result in noticeable changes in the observed behavior but detailed micro-PL experiments could probably highlight this question.

In conclusion, we have presented a semiconductor disordered system where localized excitonic states clearly exist above the demarcation energy, which otherwise might be regarded as an effective excitonic mobility edge. We suggest that the driving force of the observed intricate peculiarities is a macroscopic modulation of the intrinsic microscopic random potential, resulting most probably from random coupling between 2D islands, laterally extended on the scale of the excitonic diffusion length. Similar effects may be of crucial importance for understanding localization dynamics in different technologically important semiconductor structures involving self-ordering effects on the macroscopic scale.<sup>26</sup>

This work has been supported in part by the RFBR and by the Program of Ministry of Science of RF “Physics of Solid State Nanostructures.” The authors acknowledge the expert help of Dr. I. Ivanov from Linköping University in the selective excitation PL measurements.

- 
- <sup>1</sup>N. F. Mott and E. A. Davis, *Electronic Processes in Non-Crystalline Materials*, 2nd ed. (Oxford University Press, Oxford, England, 1979).
- <sup>2</sup>E. Cohen and M. D. Sturge, *Phys. Rev. B* **25**, 3828 (1982).
- <sup>3</sup>J. Hegarty, L. Goldner, and M. D. Sturge, *Phys. Rev. B* **30**, 7346 (1984).
- <sup>4</sup>S. Permogorov, A. Reznitsky, V. Travnikov, S. Verbin, G. O. Mueller, P. Floegel, and M. Nikiforova, *Phys. Status Solidi B* **106**, K57 (1981).
- <sup>5</sup>D. Gershoni, E. Cohen, and A. Ron, *Phys. Rev. Lett.* **56**, 2211 (1986).
- <sup>6</sup>A. A. Klochikhin, S. A. Permogorov, and A. N. Reznitskii, *Phys. Solid State* **39**, 1035 (1997).
- <sup>7</sup>A. Satake, Y. Masumoto, T. Miyajima, T. Asatsuma, F. Nakamura, and M. Ikeda, *Phys. Rev. B* **57**, R2041 (1998).
- <sup>8</sup>H. Kalt, J. Collet, S. D. Baranovskii, R. Saleh, P. Thomas, Le Si Dang, and J. Cibert, *Phys. Rev. B* **45**, 4253 (1992).
- <sup>9</sup>R. P. Stanley, J. P. Doran, J. Hegarty, and R. D. Feldman, *Physica B* **191**, 71 (1993).
- <sup>10</sup>U. Jahn, M. Ramsteiner, R. Hey, H. T. Grahn, E. Runge, and R. Zimmermann, *Phys. Rev. B* **56**, R4387 (1997).
- <sup>11</sup>L. E. Golub, S. V. Ivanov, E. L. Ivchenko, T. V. Shubina, A. A. Toropov, J. P. Bergman, G. R. Pozina, B. Monemar, and M. Willander, *Phys. Status Solidi B* **205**, 203 (1998).
- <sup>12</sup>A. Chomette, B. Deveaud, A. Regreny, and G. Bastard, *Phys. Rev. Lett.* **57**, 1464 (1986).
- <sup>13</sup>P. S. Kop'ev, R. A. Suris, I. N. Uraltsev, and A. M. Vasiliev, *Solid State Commun.* **72**, 401 (1989).
- <sup>14</sup>K. Fujiwara, N. Tsukada, T. Nakayama, and A. Nakamura, *Phys. Rev. B* **40**, 1096 (1989).
- <sup>15</sup>S. Jackson, W. E. Hagston, T. J. Gregory, J. Goodwin, J. E. Nicholls, J. H. C. Hogg, B. Lunn, and D. E. Ashenford, *J. Cryst. Growth* **117**, 867 (1992).
- <sup>16</sup>T. Amand, J. Barrau, X. Marie, N. Lauret, B. Dareys, M. Brousseau, and F. Laruelle, *Phys. Rev. B* **47**, 7155 (1993).
- <sup>17</sup>S. V. Ivanov, S. V. Sorokin, I. L. Krestnikov, N. N. Faleev, B. Ya. Ber, I. V. Sedova, and P. S. Kop'ev, *J. Cryst. Growth* **184/185**, 70 (1998).
- <sup>18</sup>S. V. Ivanov, A. A. Toropov, T. V. Shubina, S. V. Sorokin, A. V. Lebedev, I. V. Sedova, P. S. Kop'ev, G. R. Pozina, J. P. Bergman, and B. Monemar, *J. Appl. Phys.* **83**, 3168 (1998).
- <sup>19</sup>A. A. Toropov, S. V. Ivanov, T. V. Shubina, A. V. Lebedev, S. V. Sorokin, P. S. Kop'ev, G. R. Pozina, J. P. Bergman, and B. Monemar, *J. Cryst. Growth* **184/185**, 293 (1998).
- <sup>20</sup>The SL period and average amount of CdSe located in the layers were determined by simulating the rocking curves measured for different symmetric and asymmetric reflexes. More details of the analysis will be published elsewhere.
- <sup>21</sup>A. Toropov, S. V. Ivanov, T. V. Shubina, S. V. Sorokin, A. V. Lebedev, A. A. Sitnikova, P. S. Kop'ev, M. Willander, G. Pozina, J. P. Bergman, and B. Monemar, *Jpn. J. Appl. Phys. Part 1* (to be published).
- <sup>22</sup>Z. Zhu, H. Yoshihara, K. Takebayashi, and T. Yao, *Appl. Phys. Lett.* **63**, 1678 (1993).
- <sup>23</sup>U. Neukirch, D. Weckendrup, W. Fashinger, P. Juza, and H. Sitter, *J. Cryst. Growth* **138**, 849 (1994).
- <sup>24</sup>M. Umlauff, J. Hoffmann, H. Kalt, W. Langbein, J. M. Hvam, M. Sholl, J. Söllner, M. Heuken, B. Jobst, and D. Hommel, *Phys. Rev. B* **57**, 1390 (1998).
- <sup>25</sup>S. Permogorov, A. Reznitsky, L. Tenishev, A. Kornievsky, S. Ivanov, S. Sorokin, M. Maximov, I. Krestnikov, W. von der Osten, H. Stolz, M. Jütte, and H. Vogelsang, in *Proceedings of the 23rd International Conference on the Physics of Semiconductors, Berlin, Germany, 1996*, edited by M. Scheffler and R. Zimmermann (World Scientific, Singapore, 1996), p. 2015.
- <sup>26</sup>J. Tersoff, C. Teichert, and M. G. Lagally, *Phys. Rev. Lett.* **76**, 1675 (1996).